Kerr Effect in Liquid Helium at Temperatures Below the Superfluid Transition

A. O. Sushkov,[1,2,*] E. Williams,[1,†] V. V. Yashchuk,[1,‡] D. Budker,[1,3,§] and S. K. Lamoreaux[2,∥]

[1]*Department of Physics, University of California at Berkeley, Berkeley, California 94720-7300, USA*
[2]*Los Alamos National Laboratory, Physics Division 23, University of California, M.S. H803, Los Alamos, New Mexico 87545, USA*
[3]*Nuclear Science Division, Lawrence Berkeley National Laboratory, Berkeley, California 94720, USA*
(Received 30 March 2004; published 6 October 2004)

The electro-optical Kerr effect induced by a slowly varying electric field in liquid helium at temperatures below the λ point is investigated. The Kerr constant of liquid helium is measured to be $(1.43 \pm 0.02^{(stat)} \pm 0.04^{(sys)}) \times 10^{-20}$ (cm/V)^2 at $T = 1.5$ K. Within experimental uncertainty, the Kerr constant is independent of temperature in the range $T = 1.5$ K to 2.17 K, which implies that the Kerr constant of the superfluid component of liquid helium is the same as that of normal liquid helium. Pair and higher correlations of He atoms in the liquid phase account for about 23% of the measured Kerr constant. Liquid nitrogen was used to test the experimental setup; the result for the liquid nitrogen Kerr constant is $(4.38 \pm 0.15) \times 10^{-18}$ (cm/V)^2. Kerr effect can be used as a noncontact technique for measuring the magnitude and mapping out the distribution of electric fields inside these cryogenic insulants.

The electro-optical Kerr effect describes birefringence induced in an initially isotropic medium by an externally applied electric field $\vec{E}$ [1,2]. Linearly polarized light propagating in such a medium experiences a different index of refraction when its polarization is parallel to $\vec{E}$ compared to the case when its polarization is perpendicular to $\vec{E}$. The difference between the two refractive indices is proportional to $|\vec{E}|^2$:

$$\Delta n = n_{\parallel} - n_{\perp} = KE^2, \tag{1}$$

where K is the Kerr constant of the material. The Kerr constant is directly related to the third-order nonlinear susceptibility.

As far as we know, the Kerr effect has not been previously observed in liquid helium. However, the value of K_{LHe} is of importance both from the fundamental and the applied viewpoints. Kerr effect measurements probe the nature of the atom distribution and atomic collisions in the medium under study. In the simplest approximation of noninteracting spherically symmetric atoms, the Kerr constant is due to the hyperpolarizability γ of an individual atom, and is proportional to the density of the medium: $K \propto \rho\gamma$ [3]. This is valid at low densities, and it is how the measurement of the Kerr effect in helium gas at room temperature gave $\gamma = (44.2 \pm 0.8)$ atomic units for the helium atom [4,5]. At higher densities, however, the pair-polarizability anisotropy of the van der Waals atomic complexes contributes to the Kerr constant as the second Kerr virial coefficient [6]. The second Kerr virial coefficient has never been detected for helium, although it has been measured for the noble gases Ar, Kr, and Xe [6]. At liquid densities, the atoms are so close together that polarizability anisotropies of two, three, and more atoms all contribute to the Kerr constant. An interesting question is whether the superfluidity of liquid helium has any effect on these many-body interactions and thus the Kerr

constant. Furthermore, in the neighborhood of the helium λ transition, anomalous light scattering due to fluctuations in the order parameter has been detected, see Ref. [7] for a review. We pay particular attention to the region around the λ point, looking for any anomalous behavior of the Kerr constant associated with these fluctuations.

From a more applied standpoint, the Kerr effect can be used as a noncontact way of measuring the magnitude and the distribution of electric field in systems where liquid helium is used as the insulator, such as a superconducting power apparatus [8]. Specifically, we proposed to use the Kerr effect for monitoring and diagnostics of the electric field setup in the new experiment measuring the parity- and time-reversal-invariance violating electric dipole moment of the neutron [9].

We have observed the Kerr effect in liquid helium using light of 785-nm wavelength, and measured the liquid helium Kerr constant K_{LHe} in the temperature range 1.5 K to 2.17 K at saturated vapor pressure. The apparatus
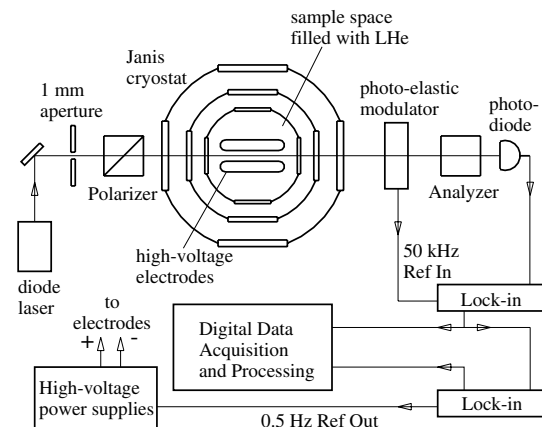

FIG. 1. A schematic top view of the experimental apparatus.

used to accomplish this is shown in Fig. 1. We use a Janis model DT SuperVariTemp pumped helium cryostat with minimum operating temperature of 1.5 K. Optical access is provided via fused quartz windows, the innermost windows having the diameter of 1/2 in. The central sample space of the cryostat, holding the liquid helium and the high-voltage electrodes, is a vertical cylinder, 2 in. in diameter. At the top of the cryostat, the sample space is connected to a Stokes Pennwalt rotary vane pump via a 3/4 in.-diameter pumping arm. Also at the top, there is a connection to an MKS Baratron Type 220B pressure gauge.

In addition, the LakeShore Silicon Diode temperature sensor, model DT-470-CU-13-1.4L (resolution 0.1 K), is mounted inside the sample space about 3 cm above the light path. LakeShore model 321 controller, combined with a wound heater mounted next to the temperature sensor, allows rough temperature control during the experiment. However, we found that recording the helium saturated vapor pressure with the MKS Baratron allows a much more accurate measurement (resolution 0.01 K) of the LHe temperature than the LakeShore temperature sensor.

An electric field is applied across two stainless steel electrodes, held together by an acrylic fixture, and submerged in liquid helium. The electrodes are held vertically, in line with the cryostat windows. Each electrode has the following dimensions: length $= 3.44$ cm, height $= 3.44$ cm, width $= 0.88$ cm. The edges and corners of the electrodes are rounded to minimize field concentration (the residual field-magnitude excess at the edges over the field in the center of the gap is $\lesssim 5\%$). The gap between the electrodes is set to $d(293 \text{ K}) = (0.284 \pm 0.001)$ cm at room temperature. On cooldown, the gap shrinks due to thermal contraction of the acrylic spacers. By illuminating the gap with a broad light beam and observing the gap image with a charged coupled device (CCD) camera, we measured the change in the gap width during a cooldown: $d(1.5 \text{ K}) = 0.270 \pm 0.003$ cm.

High voltage is generated by two Glassman power supplies (model PS/EH20N05.0 and model PS/WG-30P10). Positive voltage is applied to one of the electrodes, and negative voltage is applied to the other. Electrical contact between the electrodes and the power supplies is made through two cryogenic high-voltage cables, running from the electrodes up through the cryostat sample space to feedthroughs at the top of the cryostat. Because of the E^2 dependence of the Kerr effect, it was desirable to apply the maximum possible voltage to the electrodes while avoiding electrical breakdown in the region where the cables are in contact with helium gas, whose pressure varied from 1 atm down to zero. The other challenge in the cable design was to minimize the heat leak into the liquid helium. Therefore, the conducting portion of the cable was chosen to be a 316L Carbon steel, 0.051 in.-diameter wire. This was insulated with three layers of Teflon heat shrink tubing, each layer having 0.016 in. wall

thickness. At the top of the cryostat, each wire is attached to the feedthrough by a brass ball, then a thick layer of curing silicone glue is spread over any exposed conducting surface to provide insulation. Tests with the sample space filled with liquid helium above the λ point (under excess pressure to suppress boiling) show that our high-voltage system allows application to each electrode of voltages up to 18 kV in magnitude. With the electrodes separated by 0.27 cm, this corresponds to the electric field of 130 kV/cm. However, when the liquid helium is at a temperature below the λ point, electrical breakdown at roughly 70 kV/cm occurs between the electrodes. These observations are consistent with the dielectric strength properties of liquid helium described in the literature [8].

We use polarimetry techniques to detect the Kerr effect-induced birefringence in liquid helium given by Eq. (1). The light beam is initially polarized at $45°$ to the electric field. After passing through the liquid helium, its polarization becomes elliptical, with ellipticity

$$\epsilon = \frac{\pi}{\lambda} K_{LHe} \int E^2 dx = \frac{\pi L}{\lambda} K_{LHe}(V/d)^2. \qquad (2)$$

Here, λ is the wavelength of the light, V is the potential difference between the electrodes, d is the gap, and the integral over the path of the light beam (taking into account edge effects) is replaced by the effective electrode length L, which depends on the dimensions of the electrodes as well as their spacing. A 3D numerical simulation of the electric field in our geometry yielded the value of the effective length: $L = (3.20 \pm 0.05)$ cm.

To measure the ellipticity ϵ we use a modulation polarimeter (Fig. 1). The light source is a 785-nm Hitachi HL7851G laser diode powered by rechargeable batteries; the beam diameter is set to 1 mm by an iris and the light power in this beam is 3 mW. The polarimeter consists of a Wollaston prism polarizer, followed by a Hinds model PEM-FS4 photo-elastic modulator, the second Wollaston prism polarizer (analyzer), and the photo-diode detector. The photo-elastic modulator operates at the frequency of 50.2 kHz, the light phase modulation amplitude is $\pi/4$, and the modulation axis is parallel to the dark axis of the polarizer. The analyzer is nearly crossed with the polarizer; it is oriented so that roughly 4% of the incident light is transmitted. This decrossing angle was chosen to optimize the signal-to-noise ratio. The (nonshot) noise due to laser-intensity fluctuations scales as the square of the decrossing angle while the ellipticity signal measured by the polarimeter scales linearly with the decrossing angle, allowing such optimization. The sample, whose birefringence properties are measured, is situated between the first polarizer and the modulator. With this polarimeter, it is possible to simultaneously measure the ellipticity and the rotation introduced into the light polarization by the sample. The signal detected by the photodiode contains harmonics of the modulator frequency (50.2 kHz): the first harmonic is proportional to

the ellipticity, and the second harmonic is proportional to the rotation. We measure the ellipticity, using a Stanford Research Systems model SR844 Lock-in amplifier to detect the amplitude of the first harmonic. To calibrate, a quarter-wave plate in a precision rotation mount is inserted into the beam next to the sample and a one degree rotation of the plate introduces one degree of ellipticity into the light. The systematic error introduced by this calibration method is 2%, due mostly to the uncertainty in the retardation quality of the quarter-wave plate.

The empty polarimeter has an ellipticity noise of 10^{-7} rad/$\sqrt{\text{Hz}}$. However, when the cryostat is inserted, the laser beam passes through six windows, introducing an offset ellipticity which varies depending on the position of the laser beam on the windows. The window-induced ellipticity can be 0.2 rad or more when the beam passes near the center of the windows. We align the laser beam so that it passes close to the edge of the inside windows; this gives a minimum window-induced ellipticity of roughly 0.02 rad. When the cryostat is operating at liquid helium temperatures, this offset ellipticity drifts within a range of about 10^{-4} rad over times of hundreds of seconds. These drifts are caused by thermal gradients in the window mounts leading to varying stress applied to the window and thus to drifting window birefringence. To separate these drifts from the Kerr effect-induced ellipticity, the voltage applied to each electrode is sinusoidally modulated at the frequency of 0.5 Hz (limited by the power supplies), and the Stanford Research Systems SR830 lock-in (with the integration constant set to 10 s) is used to pick up the ellipticity signal at the modulation frequency.

The experimental setup was tested by measuring the Kerr constant of liquid nitrogen, which is more than 2 orders of magnitude larger than that of liquid helium. At $T = 73$ K, our result for the liquid nitrogen Kerr constant is: $K_{LN_2} = (4.38 \pm 0.15) \times 10^{-18}$ (cm/V)^2. This is in agreement with the published value of K_{LN_2} [10]. Experimental conditions were slightly different in that work, but rescaling the density and temperature, one obtains $K_{LN_2}(T = 73$ K$) = 4.32 \times 10^{-18}$ (cm/V)^2 from Ref. [10] (no experimental error is given).

In liquid helium, as in liquid nitrogen, the Kerr effect was detected by measuring the light ellipticity ϵ as a function of the applied voltage V; their relationship is given by Eq. (2). The experimental results at $T = 1.5$ K are shown in Fig. 2. A quadratic fit gives the value of the liquid-helium Kerr constant:

$$K_{LHe} = (1.43 \pm 0.02^{(\text{stat})} \pm 0.04^{(\text{sys})}) \times 10^{-20} \ (\text{cm/V})^2.$$

The systematic error is the combination of errors in the electrode gap, the effective electrode length, and the ellipticity calibration method. The statistical error is due to window-ellipticity drifts, and is determined by the integration time for each point.
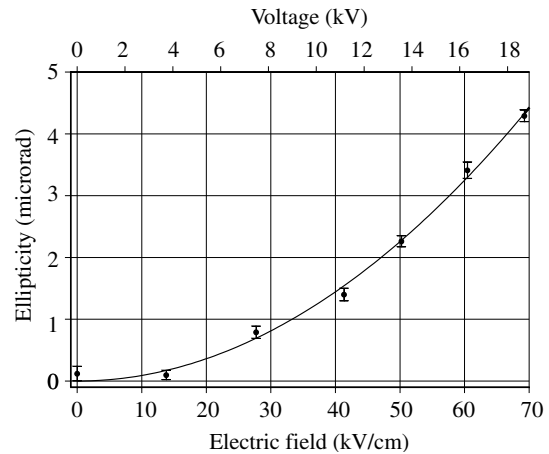
FIG. 2. The Kerr effect in liquid helium at $T = 1.5$ K: induced ellipticity as a function of the electric field between the electrodes. Integration time for each point is 1000 s. Potential difference between the electrodes is shown on the upper scale. Larger electric fields were not applied because of breakdown in liquid helium.

It is interesting to compare this number with the Kerr constant expected from the value of the helium atom hyperpolarizability: $\gamma = (44.2 \pm 0.8)$ atomic units, deduced from the measurement of the Kerr effect in the helium gas at room temperature [4]. The contribution of the hyperpolarizability of the individual helium atoms to the Kerr constant of the liquid at $T = 1.5$ K is $K_{LHe}^{(0)} = (1.10 \pm 0.02) \times 10^{-20}$ (cm/V)^2 [11]. There is another density-dependent contribution to K_{LHe}, due to the polarizability anisotropy of van der Waals complexes of two or more helium atoms in the external electric field. To our knowledge, this contribution has not been measured for an atomic liquid. Some theoretical calculations have been performed, predicting that for liquid argon, the contribution due to van der Waals complexes is a factor of 9 greater than the hyperpolarizability contribution [12]. The conclusion from our experimental result for K_{LHe} is that in liquid helium, the contribution due to van der Waals complexes is a factor of 3 less than the hyperpolarizability contribution. We performed a naive estimate of the pair-correlation effect, using the pair-polarizability anisotropy of a He$_2$ dimer in the dipole-induced-dipole approximation, and obtained the right sign and order of magnitude for the contribution to the liquid-helium Kerr constant from the pair interactions between the helium atoms.

The temperature dependence of the liquid-helium Kerr constant was measured in the range starting at the minimum temperature achievable in the LakeShore cryostat, $T = 1.5$ K, and up to the λ point, $T = 2.17$ K. As seen from Fig. 3, within the experimental error, the Kerr constant does not depend on temperature in this range. This is due, in part, to the fact that the density of liquid helium changes by only 0.7% in this temperature range [13]. However, it should also be noted that, in the two-
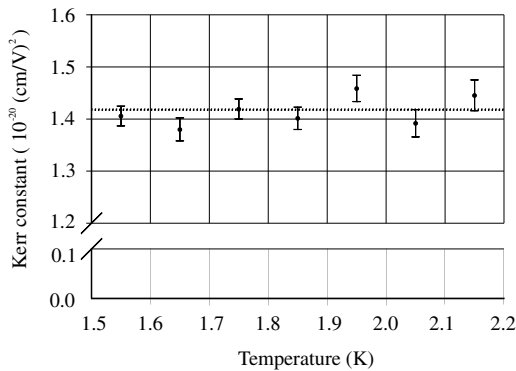
FIG. 3.   The liquid helium Kerr constant in the temperature range $T = 1.5$ K to $T = 2.17$ K. The electric field between the electrodes is 69 kV/cm, and the temperature is scanned up or down. Each point on the graph is obtained by averaging the Kerr effect-induced ellipticity readings over the interval of 0.1 K. The dashed line indicates the average over all the points, which agrees with the value of K_{LHe} given in the text.

fluid model, the fraction of the total density that is in the superfluid component changes from zero at the λ point to about 90% at 1.5 K. The absence of temperature dependence in Fig. 3 means that, within our experimental accuracy, the Kerr constant of the superfluid component of liquid helium is the same as that of the normal component. Furthermore, no anomalous temperature dependence in the vicinity of the λ point could be seen during the experiment.

No reliable data could be obtained for K_{LHe} above the λ transition. There are several experimental difficulties encountered when trying to detect the Kerr effect in liquid helium above the superfluid transition. These are mostly associated with its low thermal conductivity. Below the λ point, LHe is a nearly perfect thermal conductor [14]; therefore, there is no thermal convection or boiling, so the laser beam going through it is undisturbed. Normal liquid helium, however, is a very poor thermal conductor ($\kappa \approx 2 \times 10^{-4}$ W/cm $\cdot$ K). Even though, to prevent boiling, we kept the pressure in the cryostat sample space at 1.3 atm, while performing Kerr-effect measurements above the λ point, the laser beam was still significantly distorted on its passage through LHe, making the data unreliable. A possible explanation for this is as follows. Because of the low thermal conductivity and viscosity, thermal gradients in normal liquid helium create convection currents and density gradients which are responsible for the scattering and distortion of the laser beam. In fact, this scattering is the basis for optical visualization techniques used for imaging convective flow patterns in liquid helium [15].

In conclusion, we have measured the Kerr constant of liquid helium to be $(1.43 \pm 0.02^{(\text{stat})} \pm 0.04^{(\text{sys})}) \times 10^{-20}$ (cm/V)^2 at $T = 1.5$ K and showed that, within the experimental uncertainty, it has no temperature de-

pendence in the range $T = 1.5$ K to 2.17 K. The measured value of K_{LHe} indicates that in the liquid phase, the polarizabilities of van der Waals complexes of He atoms account for approximately 23% of the experimentally measured Kerr constant. The absence of temperature dependence suggests that, within the achieved precision, superfluidity has no effect on the Kerr constant of liquid helium. Finally, the measurement of K_{LHe} allows the use of Kerr effect as a nonintrusive technique for measuring the magnitude and mapping out the distribution of electric fields inside superfluid liquid helium.

*Electronic address: alex000@socrates.berkeley.edu
†Electronic address: ewilliam@uclink.berkeley.edu
‡Electronic address: yashchuk@socrates.berkeley.edu
§Electronic address: budker@socrates.berkeley.edu
‖Electronic address: lamore@lanl.gov

[1] J. Kerr, Philos. Mag. **50**, 337 (1875).
[2] J. Kerr, Philos. Mag. **50**, 446 (1875).
[3] A. D. Buckingham and J. A. Pople, Proc. Phys. Soc. London, Sect. A **68**, 905 (1955).
[4] R. Tammer, K. Loblein, K. H. Peting, and W. Huttner, Chem. Phys. **168**, 151 (1992).
[5] L. L. Boyle, A. D. Buckingham, R. L. Disch, and D. A. Dunmur, J. Chem. Phys. **45**, 1318 (1966).
[6] A. D. Buckingham and D. A. Dunmur, Trans. Faraday Soc. **64**, 1776 (1968).
[7] W. F. Vinen and D. L. Hurd, Adv. Phys. **27**, 533 (1978).
[8] J. Gerhold, Cryogenics **38**, 1063 (1998).
[9] LANSCE Neutron EDM Experiment, http://p25ext.lanl.gov/edm/edm.html.
[10] K. Imai, A. Kanematsu, M. Nawata, and M. Zahn, in *Proceedings of the 3rd International Conference on Properties and Applications of Dielectric Materials* (Cat. No. 91CH2937-1), (IEEE, New York, NY, 1991), Vol. 1, pp. 280-283.
[11] We neglect the density dependence of γ, since, from the results of H. Koch *et al.*, J. Chem. Phys. **111**, 10108 (1999), the correction is on the order of or less than the experimental uncertainty.
[12] J. A. Brace and J. V. Champion, J. Phys. C **2**, 2408 (1969).
[13] K. R. Atkins, *Liquid Helium* (Cambridge University Press, Cambridge, England, 1959).
[14] F. Pobell, *Matter and Methods at Low Temperatures* (Springer, Berlin, 1996).
[15] A. L. Woodcraft, P. G. J. Lucas, R. G. Matley, and W. Y. T. Wong, J. Low Temp. Phys. **114**, 109 (1999).